Article:
Durkie, M., Chong, J., Valluru, M.K. et al. (2 more authors) (2021) Biallelic inheritance of hypomorphic PKD1 variants is highly prevalent in very early onset polycystic kidney disease. Genetics in Medicine, 23 (4). pp. 689-697. ISSN 1098-3600

https://doi.org/10.1038/s41436-020-01026-4

Biallelic inheritance of hypomorphic *PKD1* variants is highly prevalent in very early onset polycystic kidney disease

Miranda Durkie FRCPath[1], Jiehan Chong MRCP[2], Manoj K Valluru PhD[2], Peter C Harris PhD[3], Albert CM Ong DM, FRCP[2]

[1]Sheffield Diagnostics Genetic Service, Sheffield Children's NHS Foundation Trust, Sheffield, UK

[2] Kidney Genetics Group, Academic Nephrology Unit, Department of Infection, Immunity and Cardiovascular Disease, University of Sheffield Medical School, Sheffield, UK

[3] Division of Nephrology and Hypertension, Mayo Clinic and Foundation, Rochester, USA

Correspondence:

Prof Albert CM Ong

Kidney Genetics Group, Academic Nephrology Unit, Department of Infection, Immunity and Cardiovascular Disease, University of Sheffield Medical School, Sheffield, UK

0114 215 9542

a.ong@sheffield.ac.uk

Conflict of interest statement

The authors declare no conflicts of interest.

Abstract

Purpose

To investigate the prevalence of biallelic *PKD1* and *PKD2* variants underlying very early onset (VEO) polycystic kidney disease in a large international paediatric cohort referred for clinical indications over a 10-year period (2010-2020).

Methods

All samples were tested by Sanger sequencing and MLPA of *PKD1* and *PKD2* genes and/or a next-generation sequencing panel of 15 additional cystic genes including *PKHD1* and *HNF1B*. Two patients underwent exome or genome sequencing.

Results

Likely causative *PKD1 or PKD2* variants were detected in 30 infants with PKD-VEO, 16 of whom presented *in utero*. 21/30 (70%) had two variants with biallelic *in trans* inheritance confirmed in 16/21, 1 infant had biallelic *PKD2* variants and 2 infants had digenic *PKD1/PKD2* variants. There was no known family history of ADPKD in 13 families (43%) and a *de novo* pathogenic variant was confirmed in 6 families (23%).

Conclusion

We report a high prevalence of hypomorphic *PKD1* variants and likely biallelic disease in infants presenting with PKD-VEO with major implications for reproductive counselling. The diagnostic interpretation and reporting of these variants however remains challenging using current ACMG/AMP and ACGS variant classification guidelines in PKD-VEO and other diseases affected by similar variants with incomplete penetrance.

Key words: PKD1, PKD2, VEO, hypomorphic, ACMG

Introduction

Autosomal dominant polycystic kidney disease (ADPKD) is the most common genetic cause of kidney failure and usually presents in adult life [1]. Very rarely, ADPKD can be diagnosed *in utero* or in infancy (up to the age of 18 months) with an often severe, very early onset (VEO) presentation associated with a reported high recurrence rate in subsequent pregnancies [2].

The genetic mechanism underlying a VEO presentation has been shown to be related to reduced gene dosage [3] with biallelic *PKD1* variants being the most consistent finding in several clinical case reports [4 5 6 7]. In one study, digenic variants of *PKD1* were reported with *PKHD1* or *HNF1B* although these findings have not been confirmed in later studies [8]. For instance, a French case series of prenatal onset patients in 41 families with known ADPKD reported 15 biallelic *PKD1* variants but did not detect any trans-heterozygous variants in *PKD2*, *PKHD1* and *HNF1B* [9].

To determine the prevalence of these changes in an unselected cohort, we reviewed the results of all infants with a VEO presentation of polycystic kidney disease referred for diagnostic testing to a nationally accredited service laboratory in the UK over a 10-year period. Our results confirm a high prevalence of biallelic *PKD1* variants in VEO patients with an enrichment of 'hypomorphic' or reduced penetrance variants, often in heterozygosity with a pathogenic variant. In addition, we identified three cases of biallelic *PKD2* variants or trans-heterozygous *PKD1* and *PKD2* variants. Importantly, a positive family history of ADPKD was only present in 57% of families with a high rate of *de novo* variants in 23% of families with available parental samples. Although these results have major implications for reproductive counselling, the diagnostic interpretation and reporting of these variants remains challenging using current ACMG/AMP and ACGS variant classification guidelines.

Materials and methods

Study population

A retrospective review of ADPKD genetic testing referrals from 2010–2020 was performed. All patients with a recorded age of onset of cystic kidneys from prenatal up to 18 months were selected from a large cohort of patients referred to the Sheffield Diagnostic Genetics Service (SDGS) for diagnostic testing. Patients were selected by the date of birth at the time of referral and the specified age of onset of symptoms. 51 patients presenting below 18 months of age were identified. Patients with a clinical history not suggestive of ADPKD or with an alternative genetic diagnosis were subsequently excluded.

Methodology

The methodology used and genes analysed for each infant are summarised in **Table S1**. Between 2010 to 2016, genetic testing was carried out by bidirectional Sanger sequencing of all coding exons and ±25bp intron/exon boundaries of the *PKD1* and *PKD2* genes. For the duplicated region of *PKD1* (exons 1-33), *PKD1*-specific long-range PCR was performed followed by nested PCR and bi-directional sequencing to avoid the six highly homologous *PKD1* pseudogenes (primer sequences in **Table S2** and on request). Sequencing was analysed using Mutation Surveyor® software with two independent checks and included a check for pseudogene contamination.

From 2016 to 2018, long-range PCR and next-generation sequencing (NGS) of *PKD1* and *PKD2* using the IonTorrent Personal Genome Machine (PGM®) was performed. Long-range amplicons were pooled, purified, enzymatically fragmented (Ion Shear™ Plus), followed by end repair and adaptor ligation (Ion Plus Fragment Library Kit). Libraries were sequenced on 316 chip with a minimum depth of coverage of x50 for exons ±5bp and x30 for introns between ±6-25bp. In-house bioinformatics analysis was performed using the BAM and a

VCF file generated by the IonTorrent software. The pipeline used sambamba to determine coverage and ANNOVAR to obtain HGVS nomenclature of variants and their consequences. Only effects on build hg19 transcripts NM_000297 and NM_001009944 were reported with all pseudogene bases masked as N. The results were filtered to remove known benign variants from an in-house manually curated polymorphism list.

From 2018, testing evolved to the use of NGS on HiSeq 2000 with a minimum depth of coverage of x30 for exons ±5bp and x18 for introns between ±6-25bp. The designated cystic diagnostic panel comprised 17 genes associated with Polycystic Kidney Disease, Polycystic Liver Disease and Autosomal Dominant Tubulointerstitial Kidney Disease: *PKD1, PKD2, DNAJB11, GANAB, PKHD1, DZIP1L, PRKCSH, SEC63, SEC61B, SEC61A1, LRP5, ALG8, UMOD, HNF1β, REN, TSC1* and *TSC2*. Library prep was performed using SureSelectXT library system (Agilent Technologies) and custom in-house designed probes. To aid read alignment to *PKD1*, the entire sequence of exons 1-33 including all intronic sequences was included in the SureSelect bait capture. Sequencing on the Illumina HiSeq using the HiSeq Rapid SBS Kit v2 performing 2 x 108 bp paired end reads. Bioinformatics analysis based on the open source 'Best Practices' workflow by the Broad Institute which includes BWA alignment of reads to human genome build hg19, identification of variants using HaplotypeCaller and annotation from dbSNP. Variants were subsequently filtered against in-house benign polymorphism list.

2 infants (cases 4 and 28) were tested using all three methods of long-range PCR and sanger sequencing, long-range PCR with NGS on PGM® and SureSelect capture with NGS on Illumina HiSeq2000. 2 infants (cases 22 and 25) were tested by both Sanger sequencing and SureSelect NGS. The results were fully concordant.

One family (case 7) underwent trio exome sequencing using an inheritance-based, gene-agnostic approach. Another family (case 14) underwent trio whole genome sequencing via the UK 100,000 genomes project. Confirmation of the genotypes for case 7 and 14 and their parents was performed in our laboratory by long-range PCR and Sanger sequencing.

Variant interpretation

All sequence variants identified were assessed and scored according to American College of Medical Genetics / American Molecular Pathology (ACMG/AMP) [10] and the Association of Clinical Genetic Science (ACGS) best practice guidelines for the evaluation of pathogenicity and the reporting of sequence variants in clinical molecular genetics. Evaluation of pathogenicity included the use of Alamut® Visual 2.11 software, interrogation of available data from PKD mutation database (https://pkdb.mayo.edu), Human Gene Mutation Database (HGMD) Professional (https://portal.biobase-international.com/hgmd/pro) and the genome aggregation database for large exome and genome sequencing studies (https://gnomad.broadinstitute.org). Predicted evolutionary conservation *in silico* pathogenicity scores of missense variants were evaluated using REVEL[11] (a meta-tool incorporating 13 evolutionary conservation *in silico* tools) using a cut-off of >0.5 for likely pathogenicity (**Table S1**). Variants with an ACMG variant classification score of class 3, 4 or 5 were confirmed by independent Sanger sequencing including the use of long-range PCR for *PKD1* exons 1-33. Dosage analysis was performed using MRC-Holland MLPA kits P351 and P352. Variants with a classification of class 3-5 were reported to the clinician. For familial testing of known variants, two alternative primer sets were used for each amplicon to reduce the possibility of non-amplification of one allele due to single nucleotide variants (SNV) under the primer sites.

Molecular modelling of *PKD1* variants

PKD1 (6A70) 3D structures were modelled by SWISS-MODEL [12] and PHYRE2 [13] automated protein homology modelling server [14]. Because no experimental mutant PKD1 structures have been determined, we generated mutant structures by introducing individual missense variants *in silico*: missense variants were computationally modelled in UCSF Chimera 1.14 [15] by first swapping amino acids using optimal configurations in the Dunbrack rotamer library [16] and by taking into account the most probable rotameric conformation of the mutant residue. All kinds of direct interactions: polar and nonpolar, favourable and unfavorable including clashes were analysed using contacts command in UCSF Chimera 1.14 [15]. In the output, the atom-atom contacts are listed in order of decreasing VDW (van der Waals) overlap: positive where the atomic VDW spheres are intersecting, zero if just touching, negative if separated by space. The evolutionary conservation score of each amino acid of PKD1 (6A70) was determined using the ConSurf algorithm, based on the phylogenetic relationships between sequence homologues [17] [18]. The structural impact of missense variants was also analysed using Missense3D and VarSite [19] [20]. Lollipop plots were generated using the 'lollipop' mutation diagram generator [21].

Results

Between 2010-2020, a total of 1371 referrals were received for diagnostic PKD genetic testing. The majority were from the UK, with 256 patients (18.7%) referred from 17 other countries. From this cohort, we identified 51 infants with clinical onset before 18 months of age (**Figure 1**). 15 infants had an alternate genetic diagnosis confirmed, most commonly biallelic *PKHD1* pathogenic variants causing ARPKD (9 infants) or an *HNF1B* deletion (6 infants). In 6 patients, no pathogenic variants were detected in *PKD1* or *PKD2* but no further testing of additional cystogenes was requested and no confirmation of the original clinical diagnosis could be obtained.

A total of 53 variants were found in the 30/36 infants, of which 47 were unique (43 *PKD1* and 4 *PKD2*) and 14 which had not been previously published (**Table S1**). 16/30 of these infants presented *in utero* with cysts and/or enlarged echogenic kidneys visible on antenatal ultrasound scans (**Table 2**). There was no known family history of ADPKD in 13 (43%) families. In 6 out of 26 (23%) families with available parental samples, we were able to confirm a *de novo* pathogenic variant. Twenty-one infants had two putative variants. In 16 infants (73%) where parental samples were available, we confirmed biallelic *in trans* inheritance including 2 with *de novo* variants where phase was established by linkage with nearby variants (case 21) or NGS reads (case 12) (**Figure S1**). In 3 families, a *de novo* variant of unknown phase was detected. No parental samples were available for testing in the remaining 2 families.

Biallelic variants (pathogenic and hypomorphic combination)

16 infants had a pathogenic variant on one allele and a missense likely hypomorphic variant on the other allele. The pathogenic variant was inherited from an affected parent in 7 cases, from a parent with a positive family history in 2 cases, from a parent with no cysts and no family history in 1 case and was confirmed *de novo* in 4 cases. Parental samples were not available to confirm phase for 2 infants (cases 15 and 16). Inheritance of the likely hypomorphic variant was from an unaffected parent in all cases with parental samples available (27 parents with 0 cysts; 1 parent with 2 renal cysts; 2 families with unknown phase).

Biallelic variants (two hypomorphic alleles)

Five infants had 2 likely hypomorphic biallelic variants detected *in trans* (**Figure 1, Figure S1**). Two cases (case 18 and 19) were consanguineous and were homozygous for the likely variant. p.(Ser3037Leu) is novel but p.(Asn3188Ser) has been previously reported in a

different consanguineous family [4] and two other p.Asn3188 variants, p.(Asn3188Asp) and p.(Asn3188Ile) were reported in the French VEO-PKD cohort [9]. Three other cases were compound heterozygous for two likely hypomorphic variants. One parent (case 18) had 3 unilateral renal cysts (aged 26) while the remaining 9 parents had normal renal ultrasounds. Of interest, we detected 3 *PKD1* variants in 1 infant (case 13) and biallelic *PKD2* variants in another (case 5).

Digenic variants

Digenic *PKD1* and *PKD2* variants were found in 2 infants (case 8 and 16). Case 8 has biallelic variants in *PKD2* as well as a pathogenic variant in *PKD1*. Interestingly, the c.11713-2A>T *PKD1* pathogenic variant and the p.(Leu736_Asn737del) *PKD2* likely pathogenic variant were both inherited from the affected mother, who was diagnosed incidentally in her 20's. However the fetus also inherited the p.(Val909Ile) *PKD2* missense variant from the unaffected father. No additional cases with digenic inheritance of *PKD1* or *PKD2* variants and *PKHD1* or *HNF1B* were detected in the 20 infants tested for additional cystogenes.

Monoallelic variants (Genetically unresolved)

Nine infants had a single *PKD1* variant detected, 5 with cysts detected prenatally (**Figure 1**). 5/9 infants had one pathogenic variant detected: 3 infants inherited a pathogenic variant from an affected parent; 1 infant had a *de novo* pathogenic variant and 1 pathogenic variant was detected in an infant with a family history of ADPKD but no parental samples available. The remaining 4 infants had one likely hypomorphic variant inherited from the unaffected parent, concordant with the family history. In 2 of these families, there was a family history of ADPKD but the causative pathogenic variant in the affected parent had not been detected, consistent with pick-up rate of approximately 90% in adult onset cohorts [22 9]. Of the 9 infants with a single variant, 5/9 underwent further testing on an extended cystic panel. Consent for

further analysis was not available for the remaining 4 patients who had testing limited to *PKD1* and *PKD2* (3 cases) but also included *PKHD1* in one case.

In silico analysis

Although the majority of hypomorphic variants detected were unique, 5 variants were recurrent, either in our study (**Table 1**) or previously reported. We performed *in silico* modelling of these recurrent variants using a recent cryoEM structure of truncated (aa3049-4169) human PC1 complexed to PC2 [14] (**Figure 2**), complementing this with NMR modelling of PLAT binding to several putative ligands including Ca^{2+}, phosphatidylserine (PS), phosphatidylinositol-4-phosphate (PI4P) and β-arrestin [23] (**Figure 3**): p.(Arg3277Cys) Case 1, 2, 28 and [4 5 9]; p.(Arg3892His) Case 16 and 17; p.(Ile3167Phe) Case 10, 11 and [24]; p.(Asn3188Ser) Case 19 and [4]; p.(Glu4025Gly) Case 15 and [9].

Of note, the first two variants lie within the signature PLAT domain (Ile3167, Asn3188). A third residue (Arg3277), lies adjacent to a unique altered residue (Arg3269), both located in the first intracellular loop linking PLAT and the second transmembrane domain (TM2). A fourth residue (Arg3892) lies in the linker between the TOP domain and the TM S2 helix, in close proximity to a non-recurrent change (Ala3959) in the TM S3 helix. The fifth residue (Glu4025) lies in the TM S5 helix (**Figure 2**).

Three out of five variants were predicted to significantly alter the structure of the affected domain ie p.(Ile3167Phe), p.(Arg3277Cys), p.(Glu4025Gly) while the other two variants ie p.(Asn3188Ser) and p.(Arg3892His) were predicted to cause more subtle changes (**Table S3**). It was interesting to note that p.(Arg3892His) was inherited *in trans* with a second non-recurrent variant p.(Arg3959Val) in one patient (case 17) as they are in close proximity

based on structural modelling despite being in different domains: the combination could have had a more profound effect in altering protein function (**Figure 2**).

Missense3D analysis predicted that the p.(Ile3167Phe) substitution results in an altered surface cavity in the PLAT domain and could potentially affect a PS-binding pocket assigned in a previous NMR study that is important for membrane association (**Figure 3A**). [23] We noted that another altered residue Glu3121 (case 1) lies adjacent to Ile3167, forming part of the same membrane-interaction domain. Glu3121 is also part of the functional YEIL^{3123} AP2-binding motif shown to mediate PC1 internalisation [23]. Similarly, Gly3150 is localised in a protein interaction domain previously assigned by NMR [23] (**Figure 3B**). Asn3188 was not predicted to affect known ligand binding domains but could have a damaging effect on structure (**Table S3**).

Discussion

In this retrospective analysis of 30 infants with PKD-VEO referred over the past decade, we detected a high prevalence (70%) of biallelic variants, in particular *PKD1* hypomorphic variants. These findings have important implications for reproductive genetic counselling since there is a 25% recurrence risk in subsequent pregnancies if both parents are heterozygous for each variant. Around 40% of the infants in our cohort had no previous known family history of ADPKD so the occurrence of a severely affected infant will be highly traumatic for clinically unaffected parents. In this context, we found a high incidence of *de novo* pathogenic variants (23%) as well as 5 infants with two hypomorphic variants *in trans* (17%) causing PKD-VEO. Our results confirm those from a French prenatal cohort, almost all with a positive family history, subjected to more limited genetic analysis (*PKD1, PKD2, HNF1B, PKHD1*) [9]. Our detection rate however revealed twice the prevalence of biallelic *PKD1* variants (70% v 37%) and a five-fold higher incidence of *de novo PKD1* variants (23%

v 5%), reflecting the lower percentage of those with a positive family history in our cohort (60% v 95%). In contrast to a previous case series describing 8 pedigrees [8], we did not detect any infants trans-heterozygous for *PKD1* and pathogenic variants in *HNF1B* or *PKHD1* despite more extensive genetic testing in 20 infants (**Figure 1**). Other novel findings in our study were 3 cases of PKD-VEO due to biallelic *PKD2* variants and/or trans-heterozygosity for *PKD1* and *PKD2*.

Dosage effect and variability of phenotype severity

There is an emerging consensus that cyst formation in ADPKD arises primarily through a dosage-dependent mechanism centred around *PKD1* expression [25]. In typical adult-onset disease, patients with *PKD1* truncating pathogenic variants develop ESRD 15 years earlier than those with non-truncating pathogenic variants [26 27]. Secondly, informative case reports of PKD-VEO infants with biallelic inheritance of missense 'hypomorphic' *PKD1* variants in homozygosity (consanguineous) or heterozygosity with a pathogenic *PKD1* truncating variant (*in trans*) demonstrate the importance of gene dosage in determining phenotypic severity [4 5 9]. As observed in mouse studies [3], biallelic complete loss-of-function variants would be incompatible with live births and typically result in a high miscarriage rate or prenatal demise. Therefore, any likely 'hypomorphic' variants detected must retain partial or 'reduced' protein function. The high frequency of missense or in-frame deletions detected in this study and in previous papers are in keeping with this conclusion. Thirdly, patients with pathogenic variants in two new ADPKD genes, *GANAB* and *DNAJB11*, have late-onset disease associated with lower but not absent *PKD1* expression [28 29]. Our findings of biallelic variants in *PKD1* and *PKD2* are consistent with a dosage effect and their likely function in a polycystin-1/polycystin-2 protein complex and common cystogenic pathway [30]. Amongst our cohort of VEO cases, there was a range of phenotypic severity from severe, including 5 infants with neonatal demise or TOP, to prenatal onset of cysts with no reported enlargement of kidneys or hypertension. A limitation of our study is that clinical follow-up for

all cases was not possible; therefore we cannot exclude a prenatal or neonatal diagnosis of ADPKD due to ascertainment bias in cases with a family history of ADPKD (cases 3, 16, 25 and 27).

Recurrent *PKD1* hypomorphic variants

We detected the *PKD1* p.(Arg3277Cys) variant in 3 cases of PKD-VEO, being found *in trans* in 2 infants with a second hypomorphic *PKD1* allele. In total, this variant has now been reported in 6 cases of PKD-VEO making it the most common recurrent *PKD1* hypomorphic variant associated with this phenotype [4 5 9]. We also detected the variants, *PKD1* p.(Arg3892His) and p.(Ile3167Phe), each in two cases of PKD-VEO. The p.(Ile3167Phe) variant has been reported in another family with 2 VEO cases [24]. Although previously reported as a 'likely' pathogenic variant [4], it is frequent in population studies, has been found with a truncating pathogenic variant in several pedigrees (phase not established) and listed on the PKD mutation database as 'indeterminate', consistent with a hypomorphic role. p.(Arg3892His) has not been reported previously in association with PKD-VEO, although it has been detected in typical adult-onset patients [9 31]. Although rarely detected in population studies, it is still present at a higher frequency than expected for fully penetrant *PKD1* alleles. These variants illustrate the difficulty in assigning pathogenicity to potential hypomorphic variants based solely on population frequency.

The high prevalence of hypomorphic *PKD1* variants in this context presents a challenge to their interpretation. Currently, we can only infer the likely pathogenicity of the majority of hypomorphic variants from their predicted '*in silico*' effects on protein structure or function, evolutionary conservation of the altered residue, previous reported associations and low frequency in population databases. To confirm a true 'hypomorphic effect' on the *PKD1* protein, polycystin-1, functional studies will be required for individual variants. However,

there is currently no validated assay that is sufficiently sensitive, robust and readily accessible. In addition, the size and complexity of polycystin-1 makes this challenging to establish [32]. The variant p.(Arg3277Cys) is the only *PKD1* hypomorphic variant so far with unequivocal proven 'reduced' function in a genetically engineered mouse mutant (*Pkd1* RC mouse) [3]. Cellular studies have shown that p.(Arg3277Cys) leads to polycystin-1 misfolding, resulting in increased ER retention and reduced surface expression as has been shown for a few other *PKD1* missense variants [23]. Our use of structural modelling enabled some variants (although not all) to be further refined by their predicted effects on structure and function based on more recently available 3D structures of polycystin-1 and of PLAT. Not all domains currently have experimental structural information but as more structures of polycystin-1 become available, this approach could be applied more systematically [19].

Terminology, ACMG classification, and reporting

Hypomorphic variants also cause difficulty with current terminology, ACMG classification and reporting as they do not function as classic 'loss-of-function' variants causing autosomal dominant disease. The terminology is confusing due to the variable language used which ranges from 'hypomorphic' [4], 'reduced penetrance' or 'ultra-low penetrant' [33]. The ClinGen consortium Low Penetrance/Risk Allele Working Group has recently published guidelines on recommended terminology. For reduced penetrance variants, the use of the ACMG classes plus a quantitative descriptor i.e. "likely pathogenic, low penetrance" or "likely pathogenic, reduced penetrance" is recommended depending on sufficient quantitative penetrance estimates. These terms may be used for autosomal dominant disorders where the majority of carrier individuals do not develop features of the disease. However, the scenario for *PKD1* hypomorphic variants that cause cysts only when inherited *in trans* with another pathogenic or hypomorphic variant does not fall under this definition. We have therefore continued to use the term 'hypomorphic' throughout this publication classifying them by ACMG/ACGS guidelines but labelling the variants with ACMG class, adding H for likely hypomorphic allele.

Since hypomorphic alleles generally have no clinical phenotype in heterozygosity, they may be present in the general population at higher than expected frequencies. For example, the most common hypomorphic p.(Arg3277Cys) variant has been detected on 44 alleles in GnomAD (highest MAF 0.0005 or 0.05%). The other likely hypomorphic variants detected in our cohort had a lower incidence than 44 alleles in gnomAD with 2 exceptions. p.(Thr2873Ile) is present on 57 alleles in GnomAD but was inherited *in cis* with the p.(Arg2191His) variant, detected in 37 alleles in GnomAD (case 13): the number of alleles with both variants present is not presently available in GnomAD but it is possible that the combination of both *in cis* is more deleterious. The c.9499A>T p.(Ile3167Phe) variant has been reported both as an 'indeterminate' variant and observed *in trans* in another family with 2 cases of PKD-VEO [24]. However it has been detected on 340 alleles in gnomAD including 2 homozygotes (highest MAF 0.002). Nevertheless, structural modelling suggests that it is likely to be hypomorphic.

Detection of a putative hypomorphic variant confirmed *in trans* with a pathogenic variant is usually considered highly suspicious and use of the ACMG variant guidelines PM3 *(in trans)* classifier can often add sufficient weighting to shift the classification into class 4 likely pathogenic. However, the latest Clinical Genomic Resource (ClinGen) sequence variant interpretation (SVI) recommendation for PM3 requires that PM2 is applied i.e. variants are sufficiently rare in large population studies such as GnomAD. The PM2 threshold for an autosomal dominant fully penetrant disease is 0, a situation very rarely applicable to *PKD1* hypomorphic variants. However, if the PM2 threshold for *PKD1* hypomorphic variants was relaxed to a maximum of 45 alleles to align with p.(Arg3277Cys) frequency, the PM3 classifier could be used more frequently. Thus the majority of putative hypomorphic variants can only be classified presently as "variants of uncertain clinical significance" using ACMG. The difficulties in reporting these variants is clearly exemplified by the conflicting classification of the p.(Arg3277Cys) variant on both ClinVar (reported as class 2 likely

benign (1), class 4 likely pathogenic (1) and class 5 pathogenic (1) [https://www.ncbi.nlm.nih.gov/clinvar/variation/192320/] and the Human Gene Mutation Database (HGMD) [https://portal.biobase-international.com/hgmd/pro/all.php] where it is listed with conflicting support for pathogenicity.

Hypomorphic or reduced penetrant variants are not unique to *PKD1*. Many examples are being reported in other diseases such as Maturity-Onset Diabetes of Young (MODY) eg *HNF1A* [34], *RFX6* [35], *HNF4A* [36], Parkinson's disease (*VPS35* [37], *LRRK2* [38]), Retinal dystrophy (*ABCA4* [39]) and Joubert Syndrome (*SUFU* [40]). Further clarification is therefore urgently needed to aid variant interpretation and reporting. As the price of next-generation sequencing has fallen dramatically and many laboratories are now using this technology, it is imperative that classic disease information sources are updated to reflect the prevalence of hypomorphic variants and particularly the alternate inheritance pattern for *PKD1* and more rarely *PKD2*.

Acknowledgements

We are grateful to all referring clinicians and families for providing relevant clinical information especially Rodney Gilbert and Jackie Cook. We thank all the laboratory team at Sheffield Diagnostic Genetics and Mike Williamson for helpful discussion on NMR modelling. JC was supported by an Academic Clinical Fellowship from the UK National Institute of Health Research (NIHR).

Ethics Declaration

All families included in this service review consented for diagnostic genetic testing for ADPKD and/or an extended cystic kidney/liver disease panel in the UK National Health Service (NHS). All data has been de-identified.

Data availability

All methods and data including primer sequences, PCR conditions, software settings etc are available on request.

Author Contribution

Conceptualization: M.D, J.C., A.O.; Data curation: M.D, J.C.; Formal Analysis: M.D., M.V., P.H.; Investigation: M.D. J.C. M.V.; Resources: M.D., M.V., A.O.; Visualization: M.D., M.V., A.O.; Writing – original draft: M.D., J.C., M.V., A.O.; Writing – review & editing: M.D., P.H., A.O.

Figure legends

Figure 1

Summary of referrals for genetic testing in 51 infants presenting under 18 months of age between 2010-2020 and the main results. Of the 21 infants with biallelic variants, 20 were tested for other cystic genes either through a 17 gene panel, exome or genome sequencing.

Figure 2

Structural modelling of PC1 hypomorphic variants

(A) Lollipop plot showing missense variants relative to a schematic representation of the PC1 protein. Any position with a variant is indicated by a red circle, the grey bar represents the protein with the different amino acid positions (aa) and coloured boxes are specific functional domains. **(B)** Ribbon diagram of PC1 showing the representative missense variant residues in red. Dashed boxes correspond local impacts of variants on PC1 structure [14].

Interactions are labelled as black dashed lines (Pseudobonds), H-bonds are labelled in purple and Inter-atomic distances are expressed in Å.

Figure 3

NMR model of the PC1 PLAT domain with surface mapping of specific ligand-binding residues. (A) Membrane-facing side showing phosphatidylserine, PS (stick), Ca^{2+} (orange sphere). Surface representation indicating residues binding PS (light blue) and β-arrestin1/2 (pink). The key Ser3164 residue (red) which modulates PI4P and β-arrestin1/2 binding is indicated [23]. (B) Cytoplasmic-facing surface of PLAT showing a predicted protein-interaction domain (deep blue). Several residues identified to be altered in this study are labelled (orange) and mapped onto this model ie E3121, I3167, G3150 and N3188. Note the close proximity of E3121 and 13167 to the same Ca^{2+}-dependent PS binding pocket. E3121 also forms part of a functional $YEIL^{3123}$ motif involved in AP2-mediated internalisation of PC1 [23].

References

1. Ong AC, Devuyst O, Knebelmann B, Walz G, Diseases E-EWGfIK. Autosomal dominant polycystic kidney disease: the changing face of clinical management. Lancet. 2015;385(9981):1993-2002.
2. Zerres K, Rudnik-Schoneborn S, Deget F. Childhood onset autosomal dominant polycystic kidney disease in sibs: clinical picture and recurrence risk. German Working Group on Paediatric Nephrology (Arbeitsgemeinschaft fur Padiatrische Nephrologie. J Med Genet. 1993;30(7):583-588.
3. Hopp K, Ward CJ, Hommerding CJ, et al. Functional polycystin-1 dosage governs autosomal dominant polycystic kidney disease severity. The Journal of clinical investigation. 2012;122(11):4257-4273.
4. Rossetti S, Kubly VJ, Consugar MB, et al. Incompletely penetrant PKD1 alleles suggest a role for gene dosage in cyst initiation in polycystic kidney disease. Kidney Int. 2009;75(8):848-855.
5. Vujic M, Heyer CM, Ars E, et al. Incompletely penetrant PKD1 alleles mimic the renal manifestations of ARPKD. J Am Soc Nephrol. 2010;21(7):1097-1102.
6. Losekoot M, Ruivenkamp CA, Tholens AP, et al. Neonatal onset autosomal dominant polycystic kidney disease (ADPKD) in a patient homozygous for a PKD2 missense mutation due to uniparental disomy. Journal of medical genetics. 2012;49(1):37-40.
7. Ali H, Hussain N, Naim M, et al. A novel PKD1 variant demonstrates a disease-modifying role in trans with a truncating PKD1 mutation in patients with autosomal dominant polycystic kidney disease. BMC Nephrol. 2015;16:26.
8. Bergmann C, von Bothmer J, Ortiz Bruchle N, et al. Mutations in multiple PKD genes may explain early and severe polycystic kidney disease. Journal of the American Society of Nephrology : JASN. 2011;22(11):2047-2056 (Research Support, Non-U.S. Gov't).
9. Audrezet MP, Corbiere C, Lebbah S, et al. Comprehensive PKD1 and PKD2 Mutation Analysis in Prenatal Autosomal Dominant Polycystic Kidney Disease. J Am Soc Nephrol. 2016;27(3):722-729.
10. Richards S, Aziz N, Bale S, et al. Standards and guidelines for the interpretation of sequence variants: a joint consensus recommendation of the American College of Medical Genetics and Genomics and the Association for Molecular Pathology. Genet Med. 2015;17(5):405-424.
11. Ioannidis NM, Rothstein JH, Pejaver V, et al. REVEL: An Ensemble Method for Predicting the Pathogenicity of Rare Missense Variants. Am J Hum Genet. 2016;99(4):877-885.
12. Waterhouse A, Bertoni M, Bienert S, et al. SWISS-MODEL: homology modelling of protein structures and complexes. Nucleic Acids Res. 2018;46(W1):W296-W303.
13. Kelley LA, Mezulis S, Yates CM, Wass MN, Sternberg MJ. The Phyre2 web portal for protein modeling, prediction and analysis. Nat Protoc. 2015;10(6):845-858.
14. Su Q, Hu F, Ge X, et al. Structure of the human PKD1-PKD2 complex. Science. 2018;361(6406).
15. Pettersen EF, Goddard TD, Huang CC, et al. UCSF Chimera--a visualization system for exploratory research and analysis. J Comput Chem. 2004;25(13):1605-1612.
16. Shapovalov MV, Dunbrack RL, Jr. A smoothed backbone-dependent rotamer library for proteins derived from adaptive kernel density estimates and regressions. Structure. 2011;19(6):844-858.
17. Ashkenazy H, Abadi S, Martz E, et al. ConSurf 2016: an improved methodology to estimate and visualize evolutionary conservation in macromolecules. Nucleic Acids Res. 2016;44(W1):W344-350.
18. Landau M, Mayrose I, Rosenberg Y, et al. ConSurf 2005: the projection of evolutionary conservation scores of residues on protein structures. Nucleic Acids Res. 2005;33(Web Server issue):W299-302.

19. Ittisoponpisan S, Islam SA, Khanna T, Alhuzimi E, David A, Sternberg MJE. Can Predicted Protein 3D Structures Provide Reliable Insights into whether Missense Variants Are Disease Associated? J Mol Biol. 2019;431(11):2197-2212.
20. Laskowski RA, Stephenson JD, Sillitoe I, Orengo CA, Thornton JM. VarSite: Disease variants and protein structure. Protein Sci. 2020;29(1):111-119.
21. Jay JJ, Brouwer C. Lollipops in the Clinic: Information Dense Mutation Plots for Precision Medicine. PLoS One. 2016;11(8):e0160519.
22. Rossetti S, Consugar MB, Chapman AB, et al. Comprehensive molecular diagnostics in autosomal dominant polycystic kidney disease. J Am Soc Nephrol. 2007;18(7):2143-2160.
23. Xu Y, Streets AJ, Hounslow AM, et al. The Polycystin-1, Lipoxygenase, and alpha-Toxin Domain Regulates Polycystin-1 Trafficking. J Am Soc Nephrol. 2016;27(4):1159-1173.
24. Mantovani V, Bin S, Graziano C, et al. Gene Panel Analysis in a Large Cohort of Patients With Autosomal Dominant Polycystic Kidney Disease Allows the Identification of 80 Potentially Causative Novel Variants and the Characterization of a Complex Genetic Architecture in a Subset of Families. Frontiers in Genetics. 2020;11(464) (Original Research).
25. Ong AC, Harris PC. A polycystin-centric view of cyst formation and disease: the polycystins revisited. Kidney Int. 2015;88(4):699-710.
26. Cornec-Le Gall E, Audrezet MP, Chen JM, et al. Type of PKD1 mutation influences renal outcome in ADPKD. J Am Soc Nephrol. 2013;24(6):1006-1013.
27. Heyer CM, Sundsbak JL, Abebe KZ, et al. Predicted Mutation Strength of Nontruncating PKD1 Mutations Aids Genotype-Phenotype Correlations in Autosomal Dominant Polycystic Kidney Disease. J Am Soc Nephrol. 2016;27(9):2872-2884.
28. Porath B, Gainullin VG, Cornec-Le Gall E, et al. Mutations in GANAB, Encoding the Glucosidase IIalpha Subunit, Cause Autosomal-Dominant Polycystic Kidney and Liver Disease. Am J Hum Genet. 2016;98(6):1193-1207.
29. Cornec-Le Gall E, Olson RJ, Besse W, et al. Monoallelic Mutations to DNAJB11 Cause Atypical Autosomal-Dominant Polycystic Kidney Disease. Am J Hum Genet. 2018;102(5):832-844.
30. Ong ACM. Making sense of polycystic kidney disease. Lancet. 2017;389(10081):1780-1782.
31. Neumann HP, Jilg C, Bacher J, et al. Epidemiology of autosomal-dominant polycystic kidney disease: an in-depth clinical study for south-western Germany. Nephrol Dial Transplant. 2013;28(6):1472-1487.
32. Cai Y, Fedeles SV, Dong K, et al. Altered trafficking and stability of polycystins underlie polycystic kidney disease. J Clin Invest. 2014;124(12):5129-5144.
33. Cornec-Le Gall E, Torres VE, Harris PC. Genetic Complexity of Autosomal Dominant Polycystic Kidney and Liver Diseases. J Am Soc Nephrol. 2018;29(1):13-23.
34. Misra S, Hassanali N, Bennett AJ, et al. Homozygous Hypomorphic HNF1A Alleles Are a Novel Cause of Young-Onset Diabetes and Result in Sulfonylurea-Sensitive Diabetes. Diabetes Care. 2020;43(4):909-912.
35. Patel KA, Kettunen J, Laakso M, et al. Heterozygous RFX6 protein truncating variants are associated with MODY with reduced penetrance. Nat Commun. 2017;8(1):888.
36. Laver TW, Colclough K, Shepherd M, et al. The Common p.R114W HNF4A Mutation Causes a Distinct Clinical Subtype of Monogenic Diabetes. Diabetes. 2016;65(10):3212-3217.
37. Sharma M, Ioannidis JP, Aasly JO, et al. A multi-centre clinico-genetic analysis of the VPS35 gene in Parkinson disease indicates reduced penetrance for disease-associated variants. J Med Genet. 2012;49(11):721-726.
38. Sierra M, Gonzalez-Aramburu I, Sanchez-Juan P, et al. High frequency and reduced penetrance of LRRK2 G2019S mutation among Parkinson's disease patients in Cantabria (Spain). Mov Disord. 2011;26(13):2343-2346.

39. Bauwens M, Garanto A, Sangermano R, et al. ABCA4-associated disease as a model for missing heritability in autosomal recessive disorders: novel noncoding splice, cis-regulatory, structural, and recurrent hypomorphic variants. Genet Med. 2019;21(8):1761-1771.
40. De Mori R, Romani M, D'Arrigo S, et al. Hypomorphic Recessive Variants in SUFU Impair the Sonic Hedgehog Pathway and Cause Joubert Syndrome with Cranio-facial and Skeletal Defects. Am J Hum Genet. 2017;101(4):552-563.

Table 1 Identified variants for each case including gene, cDNA & protein nomenclature, variant effect, ACMG classification and parent of origin along with relevant family history.

Case	*Gene*	cDNA Change	Predicted Protein Change	Variant Effect	ACMG class	Parent Of Origin	Family History
1	*PKD1*	c.9361G>A	p.(Glu3121Lys)	Missense	4	Paternal	No (both parents normal scans)
	PKD1	c.9829C>T	p.(Arg3277Cys)	Missense	4H	Maternal	
2	*PKD1*	c.7483T>C	p.(Cys2495Arg)	Missense	4	Maternal	Mother affected
	PKD1	c.9829C>T	p.(Arg3277Cys)	Missense	4H	Paternal	
3	*PKD1*	c.8338G>T	p.(Glu2780*)	Nonsense	5	Paternal	Father affected
	PKD1	c.9448G>A	p.(Gly3150Ser)	Missense	4H	Maternal	
4	*PKD1*	c.8362_8363ins GCCAGCGAGGAGATCGTGGCCCAGGGCAAGCGCT	p.(Ser2788Cysfs*45)	Frameshift	5	Maternal	Maternal FHx
	PKD1	c.5848G>A	p.(Val1950Met)	Missense	3H	Paternal	
5	*PKD2*	c.817_818del	p.(Leu273Valfs*29)	Frameshift	5	Paternal	Father affected
	PKD2	c.2593G>A	p.(Val865Met)	Missense	3	Maternal	
6	*PKD1*	5877_5882del	p.(Ala1961_Gln1962del)	In-frame deletion	4	Maternal	Maternal FHx
	PKD1	c.5785G>A	p.(Glu1929Lys)	Missense	3H	Paternal	
7	*PKD1*	c.6487C>T	p.(Arg2163*)	Nonsense	5	Maternal	Mother affected
	PKD1	c.9806G>A	p.(Arg3269Gln)	Missense	3H	Paternal	
8	*PKD1*	c.11713-2A>T	p.?	Splice site	5	Maternal	Mother affected
	PKD2	c.2208_2213del	p.(Leu736_Asn737del)	In-frame deletion	4	Maternal	
	PKD2	c.2725G>A	p.(Val909Ile)	Missense	3	Paternal	
9	*PKD1*	c.5482C>T	p.(Gln1828*)	Nonsense	5	Maternal	Mother affected

	PKD1	c.9714C>T	p.(=)	?Splicing	3H	Paternal	
10	*PKD1*	c.755del	p.(Pro252Argfs*38)	Frameshift	5	Paternal	Father affected
	PKD1	c.9499A>T	p.(Ile3167Phe)	Missense	3H	Maternal	
11	*PKD1*	c.10326_10356del	p.(Gly3443Serfs*20)	Frameshift	5	*de novo*	No
	PKD1	c.9499A>T	p.(Ile3167Phe)	Missense	3H	Maternal	
12	*PKD1*	6793_6794dup	p.(Arg2266Thrfs*49)	Frameshift	5	*de novo* (in trans)	No
	PKD1	c.6484C>T	p.(Arg2162Trp)	Missense	3H	Maternal	
13	*PKD1*	c.11944C>T	p.(Gln3982*)	Nonsense	5	*de novo*	No (2 small unilateral cysts in father aged 42)
	PKD1	c.6572G>A	p.(Arg2191His)	Missense	3H	Paternal	
	PKD1	c.8618C>T	p.(Thr2873Ile)	Missense			
14	*PKD1*	c.7547G>A	p.(Arg2516His)	Missense	4	*de novo*	No (both parents normal scans)
	PKD1	c.11003A>G	p.(His3668Arg)		3H	Maternal	
15	*PKD1*	c.6727_6728del	p.(Gln2243Glufs*18)	Frameshift	5	unknown	Mother affected
	PKD1	c.12074A>G	p.(Glu4025Gly)	Missense	3H	unknown	
16	*PKD2*	c.1081C>T	p.(Arg361*)	Nonsense	5	Unknown	Father affected
	PKD1	c.11675G>A	p.(Arg3892His)	Missense	3H	Unknown	
17	*PKD1*	c.11675G>A	p.(Arg3892His)	Missense	3H	Paternal	No
	PKD1	c.11876C>T	p.(Ala3959Val)	Missense	3H	Maternal	
18	*PKD1*	c.9110C>T	p.(Ser3037Leu)	Missense	3	Paternal	No (3 unilateral cysts in father age 26) consanguineous
	PKD1	c.9110C>T	p.(Ser3037Leu)	Missense	3	Maternal	
19	*PKD1*	c.9563A>G	p.(Asn3188Ser)	Missense	4H	Maternal	No (parents normal scans; consanguinuous)
	PKD1	c.9563A>G	p.(Asn3188Ser)	Missense	4H	Paternal	
20	*PKD1*	c.2878G>A	p.(Gly960Ser)	Missense	3H	Paternal (assumed)	No

	PKD1	c.9222C>G	p.(Asn3074Lys)	Missense	3H	Maternal	
21	*PKD1*	c.3739A>G	p.(Met1247Val)	Missense	3H	*de novo (in trans)*	No (parents normal scans)
	PKD1	c.8998C>T	p.(Arg3000Cys)	Missense	3H	Maternal	
22	*PKD1*	c.5014_5015del	p.(Arg1672Glyfs*98)	Frameshift	5	*de novo*	No
	-	-	-	-	-	-	
23	*PKD1*	c.12691C>T	p.(Gln4231*)	Nonsense	5	Maternal	Mother affected
	-	-	-	-	-	-	
24	*PKD1*	c.856_862del	p.(Gly287*)	Nonsense	5	Maternal	Mother affected
	-	-	-	-	-	-	
25	*PKD1*	c.7837_7839del	p.(Leu2613del)	In-frame deletion	4	Maternal	Mother affected
	-	-	-	-	-	-	
26	*PKD1*	c.6842C>A	p.(Ser2281Tyr)	Missense	4	Unknown	Father affected
	-	-	-	-	-	-	
27	*PKD1*	c.12473T>C	p.(Met4158Thr)	Missense	3H	Paternal	Mother affected
	-	-	-	-	-	-	
28	*PKD1*	c.9829C>T	p.(Arg3277Cys)	Missense	4H	Paternal	Father normal scan
	-	-	-	-	-		Mother affected
29	*PKD1*	*c.7928G>T*	p.(Arg2643Leu)	Missense	3H	Paternal	No
	-	-	-	-	-	-	
30	*PKD1*	c.1967T>A	p.(Leu656Gln)	Missense	3H	Maternal	No (parents normal scans)
	-	-	-	-	-	-	

Table 2 Table showing clinical features of the 30 infants including age of onset/referral

Case	Age at clinical presentation	Clinical information
1	Prenatal (TOP)	TOP due to bilateral enlarged echogenic kidneys; severe oligohydramnios. Hepatic ductal plate malformation on PM.
2	Prenatal	Prenatal presentation 17/40. Severe neonatal PKD, multiple bilateral cysts, hypertension, mild pulmonary hypoplasia.
3	Prenatal	Prenatal diagnosis of PKD; confirmed on postnatal scan. Bilateral.
4	Prenatal (neonatal death)	Enlarged kidneys, small bladder & oligohydramnios detected prenatally. Postnatal massively enlarged kidneys, respiratory insufficiency, severe hypertension and neonatal death. Sister has bilateral renal cysts.
5	Prenatal (TOP)	TOP. Fetal anomalies: enlarged bilateral echogenic kidneys, increased nuchal fold and prenasal oedema.
6	Prenatal	Multiple renal cysts seen on prenatal scans; high BP.
7	Prenatal (neonatal death)	Deceased fetus, large cystic kidneys, anhydramnios, increased nuchal translucency, scalp oedema and large cisterna magna on PM.
8	Neonatal	Polycystic kidneys. Incubated due to pneumothorax at delivery. Renal USS more consistent with ARPKD. Hypertensive on medication.
9	Referred age 2 months	Large cystic right kidney. Left kidney looks like PKD.
10	Prenatal	Abnormal antenatal ultrasound - large bright kidneys, reduced amniotic fluid. Postnatal renal impairment and hypertension. Relatively stable renal function- creatinine 76 (30-48).

11	Aged 18m	Polycystic kidneys diagnosed aged 1-2 years. Rapidly progressive renal failure; renal transplant aged 20.
12	Prenatal	Prenatal echogenic kidneys. Postnatally - multiple bilateral renal cysts identified. Normal growth and development.
13	Age 18m	Multiple bilateral renal cortical cysts.
14	Referred aged 12 months	Bilateral renal cysts; enlarged kidneys.
15	Neonatal	Bilateral cystic kidneys at birth. Acute kidney failure, requiring ventilatiory support due to hypoplastic lungs. Massive kidneys compromising circulation.
16	Neonatal	Bilateral renal cysts detected postnatally.
17	Prenatal	Prenatal presentation; hypertension at birth, enlarged kidneys right 7.3 cm, left 7.6cm, diffusely echogenic with loss of cortico-medullary differentiation and a number of discrete cysts bilaterally.
18	Prenatal	Prenatal bilateral multicystic kidneys; bilateral hydronephrosis. Postnatal age 5months: both kidneys grossly enlarged, hyperechoic with multiple cysts (up to 8mm).
19	Neonatal	Hypertension at birth, scans showed echogenic kidneys.
20	Age 18m	Bilateral multicystic kidneys; atypical - no renal failure; high BP.
21	Prenatal	Polycystic kidneys detected prenatally; Postnatal poor renal function; Renal transplant aged 7.
22	Age 12m	Diminished echogenicity and renal cysts with 1 macrocyst per kidney.
23	Prenatal	Prenatal bright kidneys; postnatal large kidneys with cysts; normal renal function age 2m.

24	Referred age 16m	Clinical diagnosis of PKD; Brother has bilateral kidney cysts age 6m.
25	Prenatal	Renal cysts detected prenatally.
26	Prenatal	Prenatal bilateral multicystic kidneys; postnatal bilateral multicystic & enlarged kidneys, hypertension.
27	Prenatal	Prenatal cysts, postnatally confirmed but diminished in size over time.
28	Prenatal (neonatal death)	Prenatal onset. Baby died shortly after birth. Variant identified also present in father (normal renal USS).
29	Age 2m	Multiple renal cysts age 2m; subsequent USS showed increasing number of cysts & increase in kidney size.
30	Age 2m	Presented at 2 months with bilateral large kidneys and multiple cysts, scan typical of ADPKD.

Figure 1

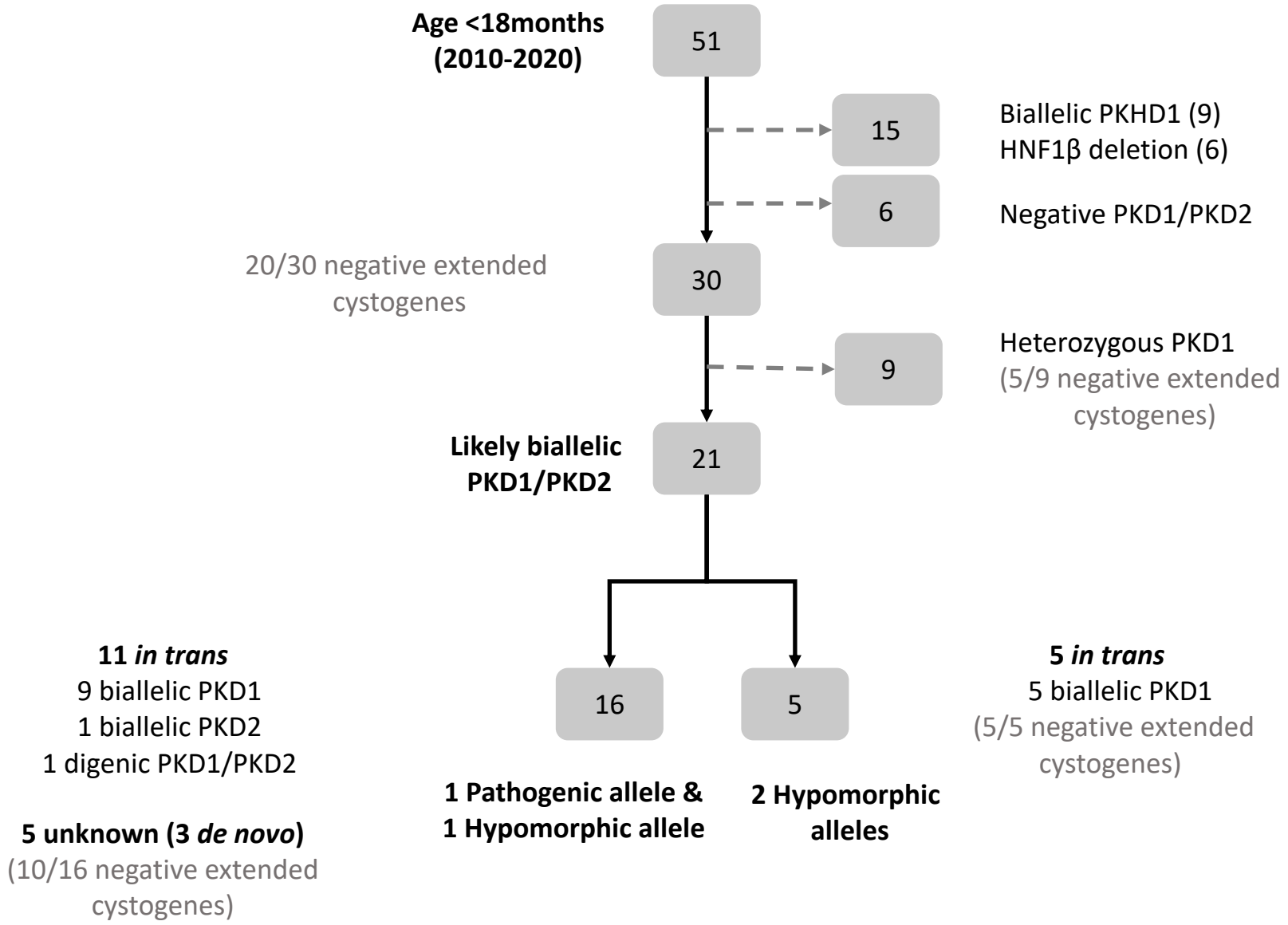
Age <18months
(2010-2020)
51
15
Biallelic PKHD1 (9)
HNF1β deletion (6)
6
Negative PKD1/PKD2
20/30 negative extended cystogenes
30
9
Heterozygous PKD1
(5/9 negative extended cystogenes)
Likely biallelic PKD1/PKD2
21
16
5
11 in trans
9 biallelic PKD1
1 biallelic PKD2
1 digenic PKD1/PKD2
5 unknown (3 de novo)
(10/16 negative extended cystogenes)
1 Pathogenic allele &
1 Hypomorphic allele
2 Hypomorphic alleles
5 in trans
5 biallelic PKD1
(5/5 negative extended cystogenes)

Figure 2

A


E3121K
G3150S
I3167F
N3188S
R3269Q
R3277C
H3668R
R3892H
A3959V
E4025G
PLAT
Polycystin cation channel
3121
3150
3188
3231
3269
3668
3711
3892
3959
4025
4113

B

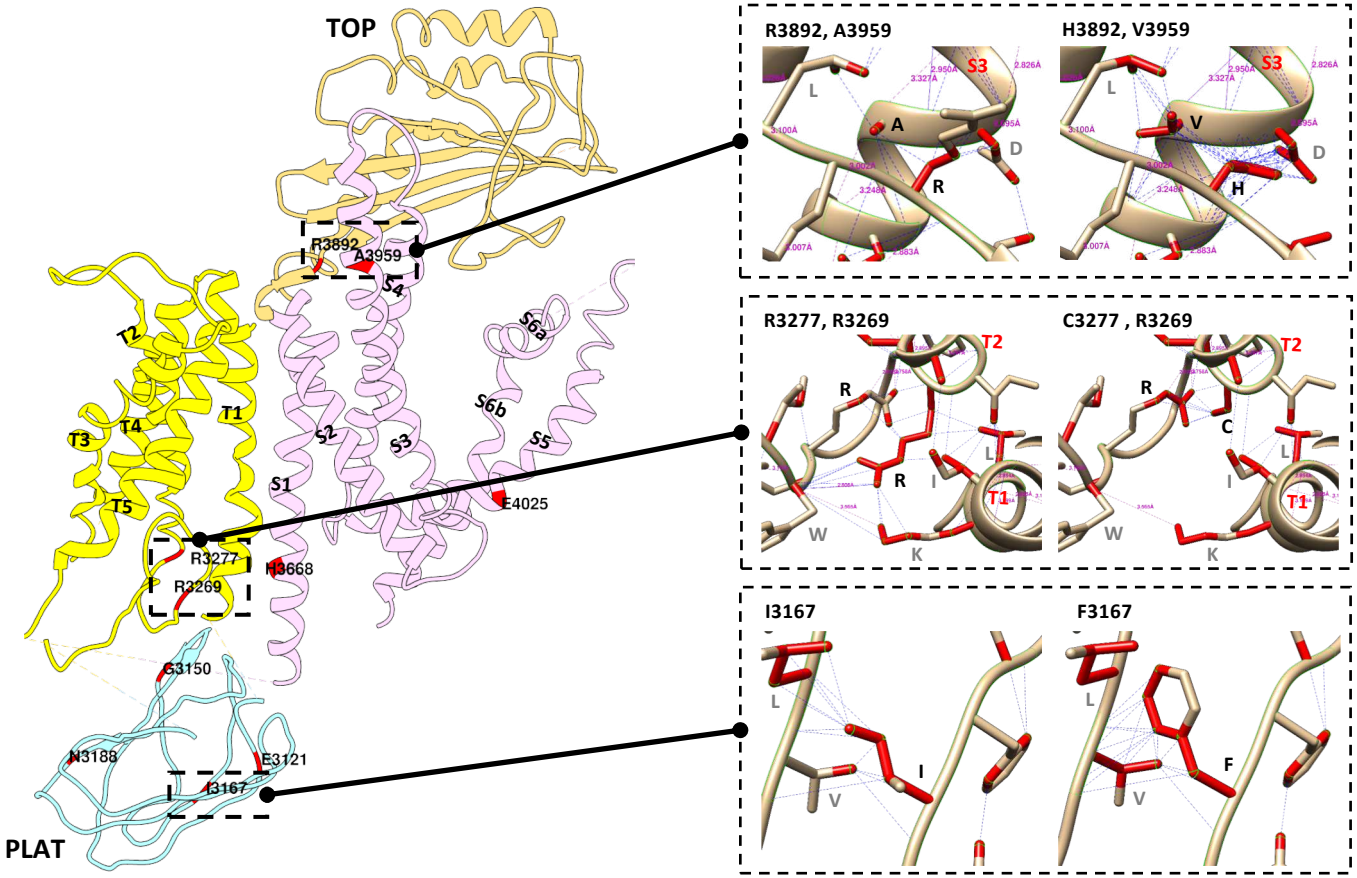
TOP
R3892
A3959
S4
T2
T1
T4
T3
T5
S1
S2
S3
S6a
S6b
S5
E4025
R3277
R3269
H3668
G3150
N3188
E3121
I3167
PLAT
R3892, A3959
H3892, V3959
R3277, R3269
C3277 , R3269
I3167
F3167

Figure 3

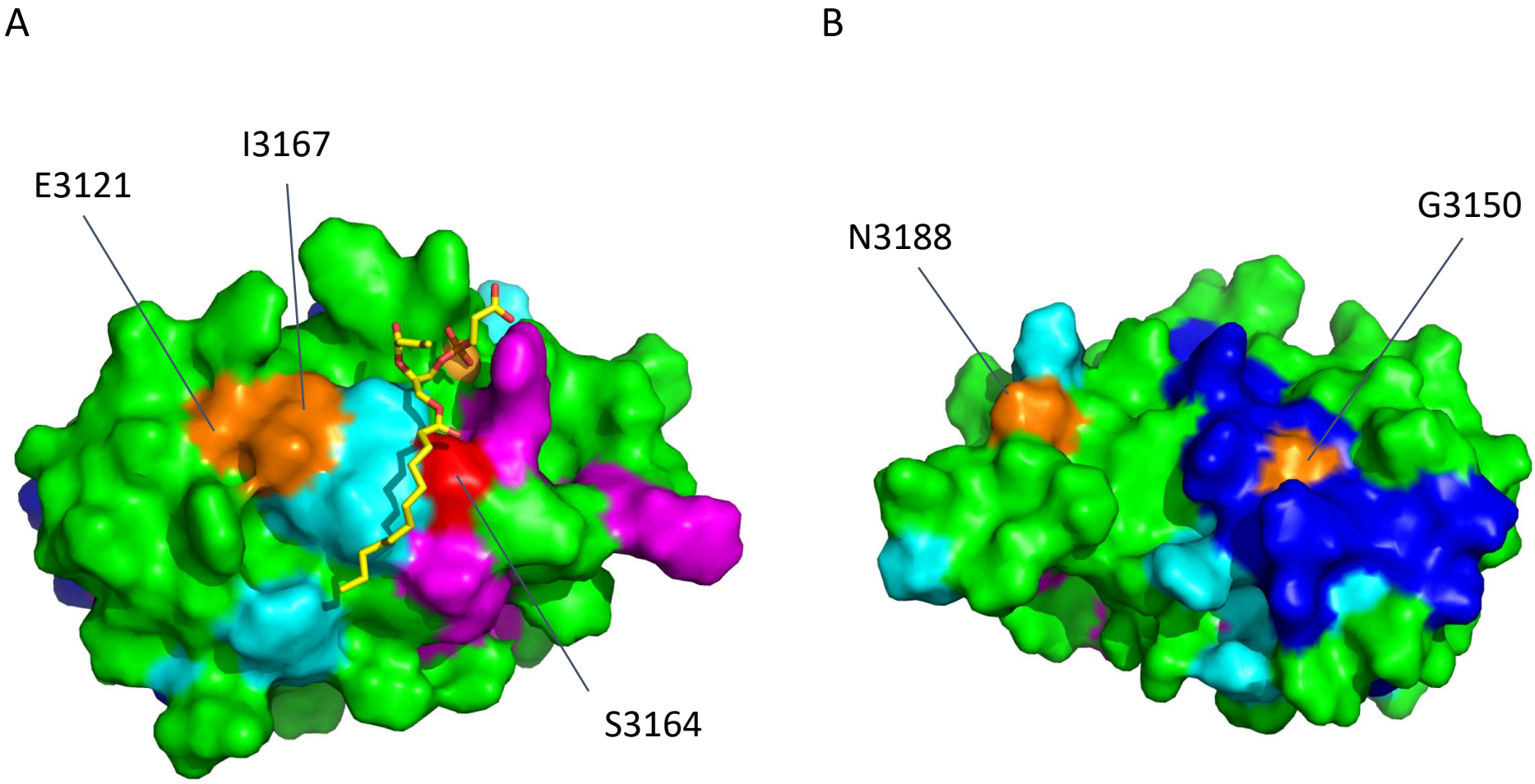

Supplementary Figures and Tables

Fig S1 The incidence of biallelic variants and their phase of transmission where available. (A) Bar chart showing the percentage of cases with a hypomorphic variant; (B) Bar chart showing phase of variants detected as determined by parental sequencing. PV: Pathogenic Variant; Hyp: Hypomorphic variant

Table S1 Table showing methodology used for each case, which genes were analysed, ACMG classification and classification evidence used. The table includes the total number of alleles with the variant detected from gnomAD v2.2.1 as well as the highest minor allele frequency (MAF) recorded in one geographical/ethnic population. REVEL score is provided for missense variants only - this evolutionary conservation *in silico* meta-tool has a cut-off of >0.5 for predicted pathogenicity. References are provided for previously reported variants.

Table S2 Table showing PKD1 long-range primer sequences. For exon 13-15F_LR a "wobble" base using IUPAC code was created to avoid non-amplification of one allele identified to cause allele drop out in 1 patient with adult-onset ADPKD. Nested primer sequences are available on request.

Table S3 In silico analysis of pathogenicity of selected variants identified using a suite of protein prediction programs.

Figure S1

A

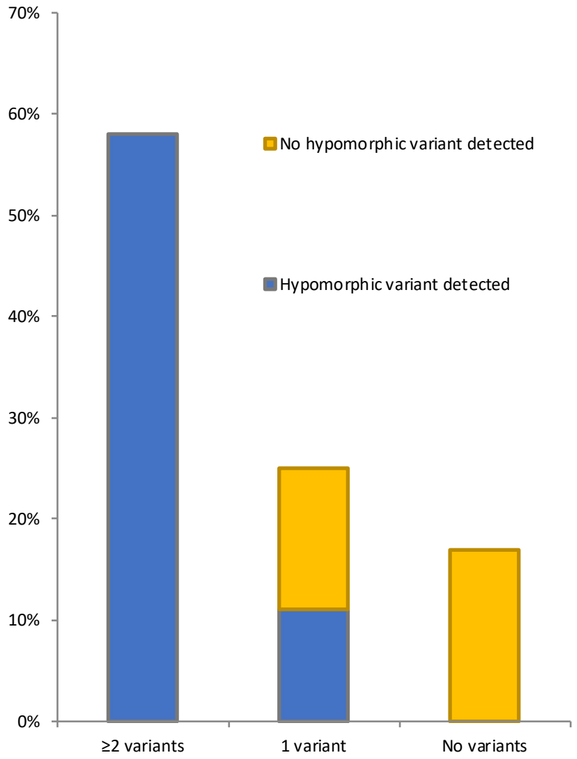
70%
60%
50%
40%
30%
20%
10%
0%
No hypomorphic variant detected
Hypomorphic variant detected
≥2 variants
1 variant
No variants

B

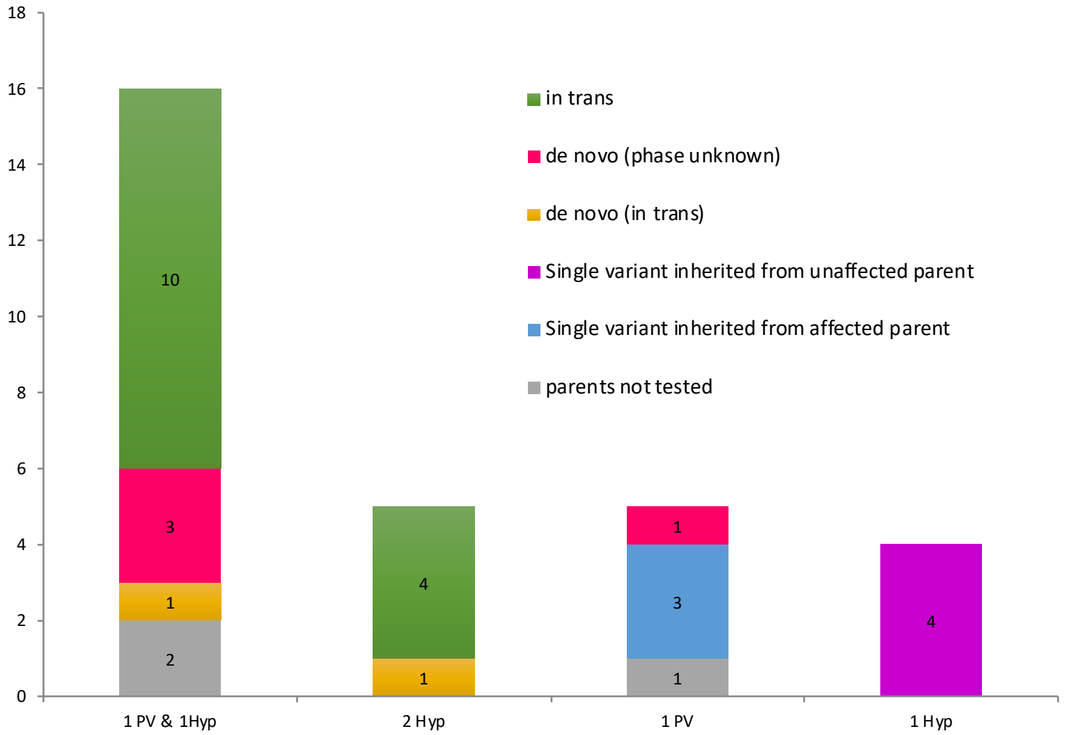
18
16
14
12
10
8
6
4
2
0
10
3
1
2
4
1
1
3
1
4
in trans
de novo (phase unknown)
de novo (in trans)
Single variant inherited from unaffected parent
Single variant inherited from affected parent
parents not tested
1 PV & 1Hyp
2 Hyp
1 PV
1 Hyp

Table S1

	Methodology	Genes tested	Gene	cDNA Change	Predicted Protein Change	Variant Effect	ACMG class	ACMG classifiers	GnomAD v2.2.1 alleles[a]	GnomAD highest MAF	REVEL score[b]	Reference
1	LR-PCR & Sanger seq	*PKD1/2*	*PKD1*	c.9361G>A	p.(Glu3121Lys)	Missense	4	PM2/PS4_mod/PP4/PM3_sup	0	n/a	0.2	Cornec-Le Gall 2013
			PKD1	c.9829C>T	p.(Arg3277Cys)	Missense	4H	PS3_mod/PS4_mod/PP1_mod/PP3/PP4	44	0.00045	0.6	Rossetti 2009
2	LR-PCR & Sanger seq	*PKD1/2*	*PKD1*	c.7483T>C	p.(Cys2495Arg)	Missense	4	PM2/PS4_mod/PP3/PP4	0	n/a	0.9	Audrezet 2012
			PKD1	c.9829C>T	p.(Arg3277Cys)	Missense	4H	PS3_mod/PS4_mod/PP1_mod/PP3/PP4	44	0.00045	0.6	Rossetti 2009
3	LR-PCR & PGM NGS	*PKD1/2*	*PKD1*	c.8338G>T	p.(Glu2780*)	Nonsense	5	PVS1/PM2/PS4_mod	0	n/a	n/a	Carrera 2016
			PKD1	c.9448G>A	p.(Gly3150Ser)	Missense	4H	PM2/PM3/PP3/PP4	2	0.000018	0.5	This study
4	LR-PCR & Sanger seq & LR-PCR & PGM NGS & SureSelect NGS	*17 gene panel*	*PKD1*	c.8362_8363ins34	p.(Ser2788Cysfs*45)	Frameshift	5	PVS1/PM2	0	n/a	n/a	Gilbert 2013
			PKD1	c.5848G>A	p.(Val1950Met)	Missense	3H	PM2/PM3/PP4	3	0.00006	0.4	Bataille 2011
5	LR-PCR & Sanger seq	*PKD1/2*	*PKD2*	c.817_818del	p.(Leu273Valfs*29)	Frameshift	5	PVS1/PM2/PS4_mod	0	n/a	n/a	Rossetti 2003
			PKD2	c.2593G>A	p.(Val865Met)	Missense	3H	PM2/PM3/PP4	1	0.000032	0.2	This study
6	SureSelect NGS	*17 gene panel*	*PKD1*	c.5877_5882del	p.(Ala1961_Gln1962del)	In-frame deletion	4	PM2/PM4/PP1_sup/PP4	0	n/a	n/a	This study
			PKD1	c.5785G>A	p.(Glu1929Lys)	Missense	3H	PM2/PM3/PP4	2	0.000057	0.2	This study
7	Exome	*Exome*	*PKD1*	c.6487C>T	p.(Arg2163*)	Nonsense	5	PVS1/PM2/PS4_mod	0	n/a	n/a	Rossetti 2001
			PKD1	c.9806G>A	p.(Arg3269Gln)	Missense	3H	PM2/PM3/PP4	1	0.000015	0.4	Kinoshita 2016
8	LR-PCR & PGM NGS	*PKD1/2; PKHD1*	*PKD1*	c.11713-2A>T	p.?	Splice site	5	PVS1/PM2	0	n/a	n/a	This study
			PKD2	c.2208_2213del	p.(Leu736_Asn737del)	In-frame deletion	4	PS4_mod/PM4/PP1_sup/PP4	26	0.00017	n/a	Stekrova 2009
			PKD2	c.2725G>A	p.(Val909Ile)	Missense	3H	PM3/PP3/PP4	21	0.00012	0.5	Athena Diag (unpublished)

9	LR-PCR & PGM NGS	*PKD1/2*	*PKD1*	c.5482C>T	p.(Gln1828*)	Nonsense	5	PVS1/PM2/PS4_mod	0	n/a	n/a	Rossetti 2002
			PKD1	c.9714C>T	p.(=)	?Splicing	3H	PM2/PM3/PP4	5	0.00022	n/a	Rossetti 2012
10	SureSelect NGS	*PKD1/2*	*PKD1*	c.755del	p.(Pro252Argfs*38)	Frameshift	5	PVS1/PM2/PS4_sup	0	n/a	n/a	Kurashige 2015
			PKD1	c.9499A>T	p.(Ile3167Phe)	Missense	3H	PS4_sup/PM3/PP3/PP4	340	0.0021	0.5	Rossetti 2002
11	LR-PCR & PGM NGS	*PKD1/2; HNF1B; TSC2*	*PKD1*	c.10326_10356del	p.(Gly3443Serfs*20)	Frameshift	5	PVS1/PM2/PM6	0	n/a	n/a	This study
			PKD1	c.9499A>T	p.(Ile3167Phe)	Missense	3H	PS4_sup/PM3/PP3/PP4	340	0.0021	0.5	Rossetti 2002
12	SureSelect NGS	*17 gene panel*	*PKD1*	c.6793_6794dup	p.(Arg2266Thrfs*49)	Frameshift	5	PVS1/PM2/PM6/PS4_sup	0	n/a	n/a	This study
			PKD1	c.6484C>T	p.(Arg2162Trp)	Missense	3H	PM3/PP4	31	0.00077	0.2	Athena Diag (unpublished)
13	LR-PCR & Sanger seq	*PKD1/2*	*PKD1*	c.11944C>T	p.(Gln3982*)	Nonsense	5	PVS1/PM2/PM6	0	n/a	n/a	Rossetti 2007
			PKD1	c.6572G>A	p.(Arg2191His)	Missense	3H	PP3/PP4	37	0.0023	0.5	Athena Diag (unpublished)
			PKD1	c.8618C>T	p.(Thr2873Ile)	Missense			57	0.00069	0.2	This study
14	WGS	*WGS*	*PKD1*	c.7547G>A	p.(Arg2516His)	Missense	4	PM2/PM6/PP3/PP4	0	n/a	0.7	Athena Diag (unpublished)
			PKD1	c.11003A>G	p.(His3668Arg)	Missense	3H	PM2/PP4/PM5_sup	0	n/a	0.2	This study
15	SureSelect NGS	*17 gene panel*	*PKD1*	c.6727_6728del	p.(Gln2243Glufs*18)	Frameshift	5	PVS1/PM2/PS4_mod	0	n/a	n/a	Rossetti 2001
			PKD1	c.12074A>G	p.(Glu4025Gly)	Missense	3H	PM2/PS4_sup/PP3/PP4	1	0.0000091	0.6	This study
16	SureSelect NGS	*17 gene panel*	*PKD2*	c.1081C>T	p.(Arg361*)	Nonsense	5	PVS1/PM2/PS4_mod	0	n/a	n/a	This study
			PKD1	c.11675G>A	p.(Arg3892His)	Missense	3H	PS4_sup/PM3_sup/PP3/PP4	17	0.00096	0.8	Neumann 2013
17	LR-PCR & Sanger seq	*PKD1/2; PKHD1; HNF1B*	*PKD1*	c.11675G>A	p.(Arg3892His)	Missense	3H	PS4_sup/PM3_sup/PP3/PP4	17	0.00096	0.8	Neumann 2013
			PKD1	c.11876C>T	p.(Ala3959Val)	Missense	3H	PP3/PP4	0	n/a	0.5	This study
18	LR-PCR & Sanger seq	*PKD1/2 PKHD1*	*PKD1*	c.9110C>T	p.(Ser3037Leu)	Missense	3H	PM2/PP4	1	0.000015	0.4	This study
			PKD1	c.9110C>T	p.(Ser3037Leu)	Missense	3H					
19			*PKD1*	c.9563A>G	p.(Asn3188Ser)	Missense	4H		0	n/a	0.7	

	SureSelect NGS	*17 gene panel*	*PKD1*	c.9563A>G	p.(Asn3188Ser)	Missense	4H	PM2/PS4_sup/PM3_sup/ PM5_sup/PP3/PP4				Rossetti 2009
20	SureSelect NGS	*17 gene panel*	*PKD1*	c.2878G>A	p.(Gly960Ser)	Missense	3H	PS4_mod/PM5_sup/PP3/ PP4	2	0.00011	0.9	Neumann 2013
			PKD1	c.9222C>G	p.(Asn3074Lys)	Missense	3H	PM2/PM6/PP4	4	0.00015	0.3	Bergmann 2011
21	LR-PCR & Sanger seq	*PKD1/2; PKHD1; HNF1B*	*PKD1*	c.3739A>G	p.(Met1247Val)	Missense	3H	PM2/PM6/PP4	0	n/a	0.4	This study
			PKD1	c.8998C>T	p.(Arg3000Cys)	Missense	3H	PM3/PS4_sup/PP4	4	0.00011	0.2	Bullich 2018
22	LR-PCR & Sanger seq & SureSelect NGS	*17 gene panel*	*PKD1* -	c.5014_5015del -	p.(Arg1672Glyfs*98) -	Frameshift -	5 -	PVS1/PS4_mod/PM6	0	n/a	n/a	Watnick 1999
23	SureSelect NGS	*PKD1/2*	*PKD1* -	c.12691C>T -	p.(Gln4231*) -	Nonsense -	5 -	PVS1/PM2/PS4_mod	0	n/a	n/a	Stekrova 2009
24	LR-PCR & Sanger seq	*PKD1/2*	*PKD1* -	c.856_862del -	p.(Gly287*) -	Nonsense -	5 -	PVS1/PM2/PS4_mod	0	n/a	n/a	O'Brien 2012
25	LR-PCR & Sanger seq & SureSelect NGS	*17 gene panel*	*PKD1* -	c.7837_7839del -	p.(Leu2613del) -	In-frame deletion -	4 -	PS4_mod/PM2/PM4_sup/ PP4	0	n/a	n/a	Bouba 2001
26	SureSelect NGS	*17 gene panel*	*PKD1* -	c.6842C>A -	p.(Ser2281Tyr) -	Missense -	4 -	PS4_sup/PM2/PM5/PP3/ PP4	0	n/a	0.9	This study
27	LR-PCR & Sanger seq & PGM NGS	*PKD1/2*	*PKD1* -	c.12473T>C -	p.(Met4158Thr) -	Missense -	3H -	PP4	31	0.0011	0.2	Athena Diag (unpublished)
28	LR-PCR & PGM NGS & SureSelect NGS	*17 gene panel*	*PKD1* -	c.9829C>T -	p.(Arg3277Cys) -	Missense -	4H -	PS3_mod/PS4_mod/PP1 _mod/PP3/PP4	44	0.00045	0.6	Rossetti 2009
29	SureSelect NGS	*17 gene panel*	*PKD1* -	c.7928G>T -	p.(Arg2643Leu) -	Missense -	3H -	PM5/PP3/PP4	19	0.00063	0.6	Garcia-Gonzalez 2007

30	LR-PCR & Sanger seq	*PKD1/2; PKHD1*	*PKD1*	c.1967T>A	p.(Leu656Gln)	Missense	3H	PS4_sup/PP4	27	0.00031	0.2	Athena Diag (unpublished)
			-	-	-	-	-					

[a] GnomAD access date 22/04/2020; [b] REVEL cut-off >0.5 used for PP3 (Ioannidis *et al* 2016)

Table S2

PKD1 long-range PCR primers	
PKD1 long-range primers	
PKD1_Ex1F_LR	AATCGCAGCCTTACCATCCACCT
PKD1_Ex1R_LR	TCATCGCCCCTTCCTAAGCATCA
PKD1_Ex2-12F_LR	CCAGCTCTCTGTCTACTCACCTCCGCATC
PKD1_Ex2-12R_LR	CTGCATCCTGTTCATCCGCTCCACGGTTAC
PKD1_Ex13-15F_LR_wobble	TGGAGGGAGGGAYGCCAATC
PKD1_Ex13-15R	AAAACACGGAAAACAGTAGATGAC
PKD1_Ex16-21F_LR	AGYGCAACTACTTGGAGGCCC
PKD1_Ex16-21R_LR	CCTGCGTTCACACAGGACAGAAC
PKD1_Ex22-34F_LR	CCGTGTAGAGAGGAGGGCGTGTGCAAGGA
PKD1_Ex22-34R_LR	TCGGCAAGGACCTGCTGGATCAGGTCTTC
PKD1_Ex34-41F_LR	TGCAGCTGGGCCCACCCTATGCCT
PKD1_Ex34-41R_LR	AGCGGGGGCCGGAGGAGTGA
PKD1_Ex42-46F_LR	GCTCGGGGACGTGGGCCTAT
PKD1_Ex42-46R_LR	TGGTGCACCCTCCGTCCCAT

Table S3

Predicted Protein Change	ConSurf	Amino acid (REF/ALT)				DynaMut	ENCoM		mCSM	SDM	Missense3D	Varsite		SIFT	Poly Phen2	PROVEAN	MA
		Polarity	Charge	Chemical	HI	ΔΔG	ΔΔG	$\Delta\Delta S_{Vib}$	ΔΔG	ΔΔG	Prediction	DP	Prediction				
p.Glu3121Lys	8	P/P	-/+	acidic/basic	-3.5/-3.9	-1.065	-0.212	0.266	-1.681	-0.03	Neutral	1.14	Favoured	0.082	1	-2.32	1.915
p.Gly3150Ser	9	NP/P	N/N	aliphatic/hydroxyl	-0.4/-0.8	-0.371	0.752	-0.94	-1.062	-0.78	Neutral	1.34	Neutral	0	1	-3.65	3.085
p.Ile3167Phe	6	NP/NP	N/N	aliphatic/aromatic	4.5/2.8	-0.353	-0.214	0.268	-0.696	-0.54	Damaging	1.13	Neutral	0.026	0.996	-2.65	2.45
p.Asn3188Ser	9	P/P	N/N	amide/hydroxyl	-3.5/-0.8	-0.344	-0.558	0.697	-0.497	-1.7	Neutral	0.66	Favoured	0	1	-4.68	2.96
p.Arg3269Gln	8	P/P	+/N	basic/amide	-4.5/-3.5	0.105	-0.35	0.438	-0.714	-1.78	Damaging	1.19	Favoured	0	1	-3.54	3.425
p.Arg3277Cys	9	P/NP	+/N	basic/sulfur	-4.5/2.5	-1.275	-0.278	0.348	-1.093	-1.82	Neutral	1.71	Unfavoured	0	1	-7.41	2.97
p.His3668Arg	8	P/P	+/+	basic/basic	-3.2/-4.5	-0.181	-0.156	0.195	-1.116	0.22	Neutral	0.81	Neutral	0.221	1	-3.24	1.895
p.Arg3892His	5	P/P	+/+	basic/basic	-4.5/-3.2	-0.825	-0.039	0.049	-1.684	0.43	Neutral	1.45	Neutral	0.143	1	-1.93	2.585
p.Ala3959Val	8	NP/NP	N/N	aliphatic/aliphatic	1.8/4.2	-0.102	0.317	-0.397	-0.63	-1.03	Neutral	0.75	Neutral	0.007	1	-1.72	2.62
p.Glu4025Gly	8	P/NP	-/N	acidic/aliphatic	-3.5/-0.4	-0.655	-0.353	0.441	-0.953	-1.55	Neutral	0.75	Unfavoured	0.003	1	-4.05	2.7

NP nonpolar, P polar, N neutral, HI Hydropathy index, ConSurf conservation scores (9 - conserved, 1 - variable), ΔΔG in kcal/mol (change in folding free energy between wild-type and mutant structures, ΔΔG ≥ 0 as stabilizing and ΔΔG < 0 as destabilizing), $\Delta\Delta S_{Vib}$ in $kcal.mol^{-1}.K^{-1}$ (Vibrational Entropy difference between wild-type and mutant structure, $\Delta\Delta S_{Vib} \geq 0$ as increase of molecule flexibility and $\Delta\Delta S_{Vib} < 0$ as decrease of molecule flexibility), DP Disease propensity value (normalized ratio of the number of disease-to-natural variants of a given type), SIFT (Score 0.0 to 0.05 is deleterious), PolyPhen-2 (Score 0.85 to 1.0 is predicted to be damaging), PROVEAN protein variation effect analyser (Score <-2.5 is deleterious), MA Mutation Assessor (Functional impact combined score).